

Implementation of a MIMO-SAR Imaging Mode for NASA's Next Generation Airborne L-Band SAR

Tobias Rommel, German Aerospace Centre (DLR), tobias.rommel@dlr.de, Germany

Rafael Rincon, National Aeronautics and Space Administration (NASA), rafael.rincon@nasa.gov, USA

Marwan Younis, German Aerospace Centre (DLR), marwan.younis@dlr.de, Germany

Gerhard Krieger, German Aerospace Centre (DLR), gerhard.krieger@dlr.de, Germany

Alberto Moreira, German Aerospace Centre (DLR), alberto.moreira@dlr.de, Germany

Abstract

Radar systems with multiple transmit and multiple receive channels (MIMO) are capable of advanced imaging modes that can benefit the next generation of Earth science and planetary science Synthetic Aperture Radar (SAR) missions. Apart from an increased flexibility, MIMO-SAR enables simultaneous full-polarized acquisitions without any reduction of the swath width or resolution. By making use of an innovative orthogonal-waveform beamforming technique, sufficient suppression of cross-correlation interference from orthogonal signals can be achieved. For verification of this MIMO-SAR imaging mode, the airborne radar sensor DBSAR-2 operated by NASA will serve as a test bed.

1 Introduction

The growing demand for high-resolution Synthetic Aperture Radar (SAR) products serves as one of the driving factors for the development of SAR systems using multiple transmit and multiple receive channels – also known as multiple-input multiple-output (MIMO) SAR. This new sensor generation enables imaging techniques that improve measurement capabilities and sets them apart from conventional SAR systems [1], [2]. One such advantageous technique is the simultaneous full-polarized SAR imaging which allows an increase of the measurement swath or a reduction of the pulse repetition frequency (PRF) with no reduction of the azimuth resolution [3]. For this purpose, the radar must transmit a pair of waveforms which are orthogonal for arbitrary shifts in time.

In [4] it was shown in very detail, that waveform orthogonality for signals covering the same frequency bands do not exist for SAR imaging in general. This is due to the time spread of the signal returns as they reflect from typically large swaths on the ground. In these cases, the echo window for the receive signal is much longer than the pulse duration itself. When making use of classical signal coding and correlation techniques, the interfering energy of the other waveforms is spread, but still completely present. To ensure signal orthogonality in SAR, it was firstly proposed in [5] to use chirp-like pseudo-orthogonal signals, which provide orthogonality only within a limited time frame. Outside this time frame, a time-variant Digital Beam-Forming (DBF) on receive is used as a spatial filter that suppresses all unwanted signals. More detailed information about this technique can be found in the next section of this paper or in [4].

When the aforementioned MIMO method is applied to polarimetry, it is possible to obtain all four parameters of the scattering matrix (HH, HV, VH, VV) within a single Pulse Repetition Interval (PRI) [3]. In this approach, chirp-like pseudo-orthogonal H and V polarized signals are transmitted simultaneously while multi-channel receivers, at each polarization, acquire and digitize the signals reflected from the ground. After digitization, time- and frequency-variant digital beam forming (DBF) is applied to the multi-channel data, at each polarization, permitting the separation of the four polarimetric components of the scattering matrix. This waveform separation approach will be referred hereafter as the orthogonal-waveform beamforming (OWB) technique, since orthogonality between the channels is achieved by the special structure of the waveform in combination with DBF [4].

The OWB technique was first verified using a ground-based MIMO-SAR demonstrator with point-like targets [6], and later in a true imaging mode with extended targets [7]. As a next step, this technique will be verified with the airborne radar sensor DBSAR-2 of the NASA Goddard Space Flight Center [8]. This radar operates at a center frequency of 1.26 GHz (L-band) and a signal bandwidth of 50 MHz. The radar employs a MIMO architecture with eight active sub-arrays in elevation, programmable arbitrary waveforms on transmit, and DBF on receive. A spacing of 10.0 cm among the radar antenna elements enables beam steering in the across-track direction over a range of approx. $\pm 45^\circ$.

The next sections of this paper are structured as follows: Section 2 describes the OWB technique and how it is used to separate the pseudo-orthogonal transmit waveforms on receive. Section 2 also includes the description of the transmit waveforms used in this study. Section 3 discuss-

es implementation and performance analysis of this technique for the DBSAR-2 sensor. Section 4 summarizes the paper and presents an outlook for future work.

2 The Orthogonal-Waveform Beam-Forming (OWB) Technique

In contrast to point target radar applications, SAR waveform orthogonality between simultaneously transmitted H and V polarizations is not only required for a single instance of time but also for arbitrary shifts between the signals due to the large time spread of the radar echo. The reason lies in the presence of the simultaneously transmitted orthogonal waveform at the output of the match filter, which degrades the quality of the SAR image. After pulse compression, those interferences are spread over time, but are still present in the SAR signal. Thus, conventional orthogonal waveforms, coding, and post processing techniques will not work properly for accurate SAR imaging. An effective way to remove the unwanted energy from the SAR waveforms is using chirp-like transmit signals with well-defined correlation characteristics, in combination with spatial filtering on receive.

One example of waveforms suitable for the OWB technique are the Segmental-Shifted Chirp (SSC) waveforms [5]. These pseudo-orthogonal waveforms are shifted versions of a chirp, which preserve the same modulation rate but require different sub-pulse durations and bandwidths. On receive, sub-pulses can be combined to a single signal of full bandwidth B and full pulse duration τ_p . An example of pseudo-orthogonal waveforms is shown in Figure 1 where a chirp and a SSC signal are plotted in the time-domain and in the time-frequency domain for two transmit channels.

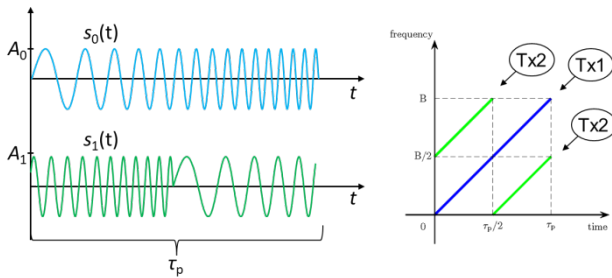


Figure 1 The Segmental-Shifted Chirp (SSC) waveforms employed in the OWB technique provide orthogonality in the return signal within a specified time frame.

Figure 2(a) shows the signal spectrum of the SSC waveform. A jump discontinuity at the center of the signal spectrum can be clearly seen. It is a result of the phase jumps in time domain at the beginning and the end of the waveform. This will lead, in turn, to a distorted impulse response after range compression, since classical tapering cannot be applied anymore. Therefore, it is suggested by

the authors to introduce a constant phase offset in the SSC transmit (Tx) waveform. If the waveform is designed with zero phase at the beginning and the end of the waveform, a discontinuity within the spectrum can be avoided (cf. Fig. 2(b)).

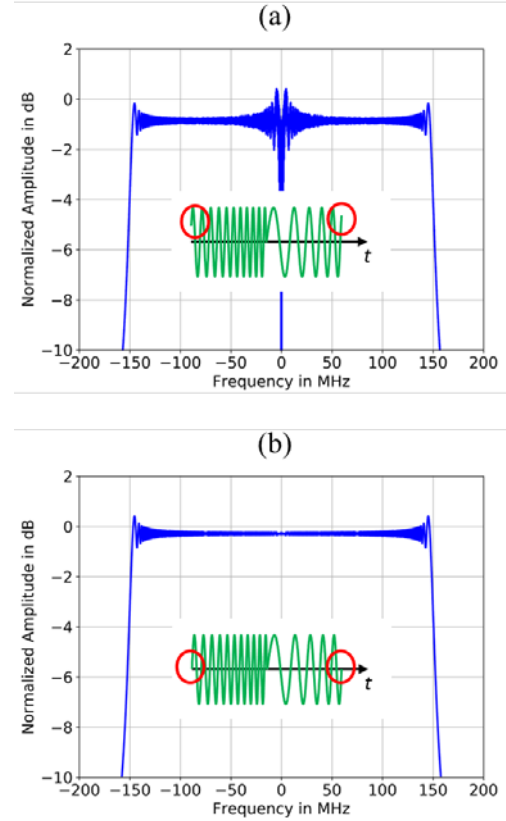


Figure 2 (a) Jump discontinuity within the signal spectrum of the second SSC waveform. (b) Second SSC waveform with constant phase offset to avoid a jump discontinuity.

As shown in Figure 1, the two waveforms are orthogonal in the time frames 0 to $\tau_p/2$ and $\tau_p/2$ to τ_p . Within these time frames the signal correlation is zero. However, when signal correlation is performed over the entire time frame 0 to τ_p , the SSC waveforms will correlate. Hence, it is necessary to form simultaneously multiple narrow receive antenna beams, each following a segment of the SSC waveforms, which effectively implement spatial filtering. However, because at each instance of time at least two segments have the same frequency content, a unique separation can still not be provided with DBF, and additional bandpass-filtering is needed. Therefore, after bandpass-filtering, the receive signals are beamformed in segments and combined in a way that two raw data streams are generated, at each of the transmitted polarizations. Hence, improved separation is achieved by effectively implementing a frequency- and time-variant antenna beams (cf. Figure 3).

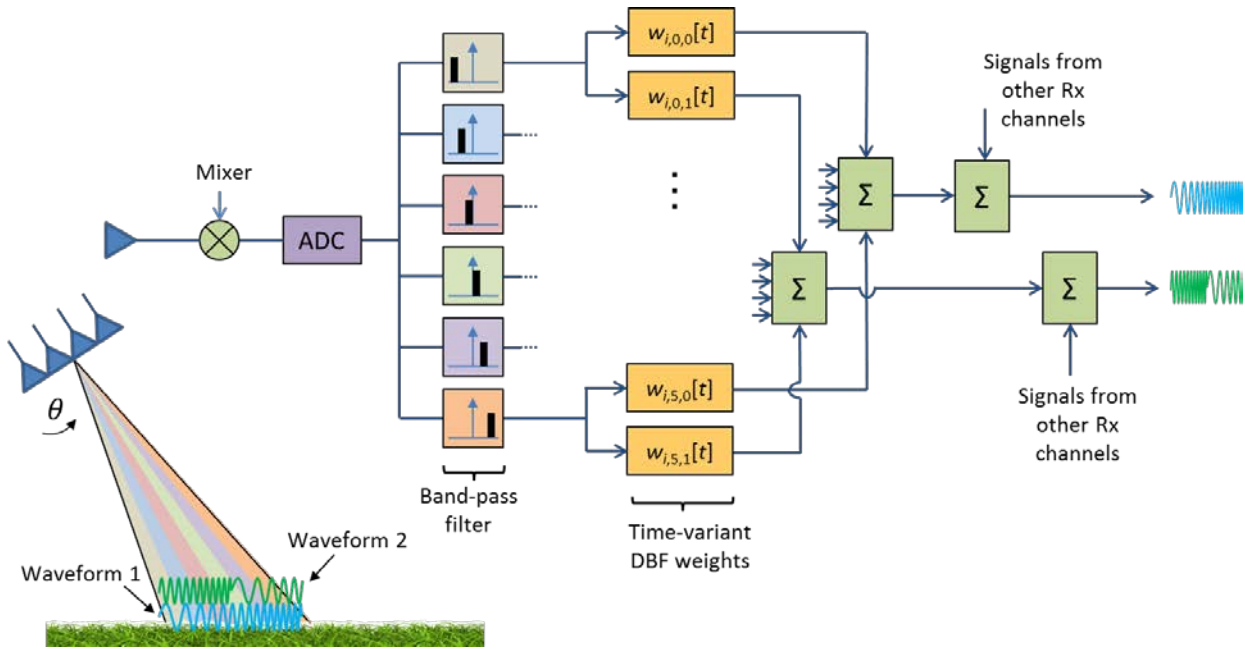


Figure 3 Post processing scheme of the orthogonal-waveform beamforming technique. After down-conversion and digitization, the echo signals pass a bank of band-pass filters and two sets of time-variant DBF weights. For illustration purposes, only a single receive channel is shown.

Alternatively, for airborne MIMO-SAR it is also possible to apply a short-time Fourier transform on the received raw-data to separate the channels – in addition to DBF. This will result in less computational complexity in comparison to the used FIR filter approach. However, for the initial implementation of the MIMO technique this elaborated idea needs for a more detailed analysis, which is foreseen for a future paper.

3 Implementation of the OWB Mode in DBSAR-2

Considering the capabilities of the DBSAR-2 radar system [8], the geometrical relations (altitude of aircraft and position of swath) and the pulse duration have been carefully chosen to ensure an optimum suppression of the interfering waveforms. On transmit, two pseudo-orthogonal waveforms with a total pulse duration of 15 μ s and a bandwidth of 50 MHz are employed for the H- and V-polarizations. The transmit waveforms are generated with constant steering weights at each of the polarizations to form a Tx beam at a 28.5° look angle, illuminating a swath between 20° ... 37° with respect to nadir. To guarantee optimum waveform suppression via DBF, the swath width must be reduced with respect to the aircraft altitude, the antenna half-power beamwidth, and the pulse duration. At an aircraft altitude of 3.0 km, this leads to a swath width of 529 m. This is, in fact, a relatively narrow swath for MIMO-SAR imaging but sufficient to demonstrate the capability and benefits of the OWB technique for future implementation in spaceborne systems.

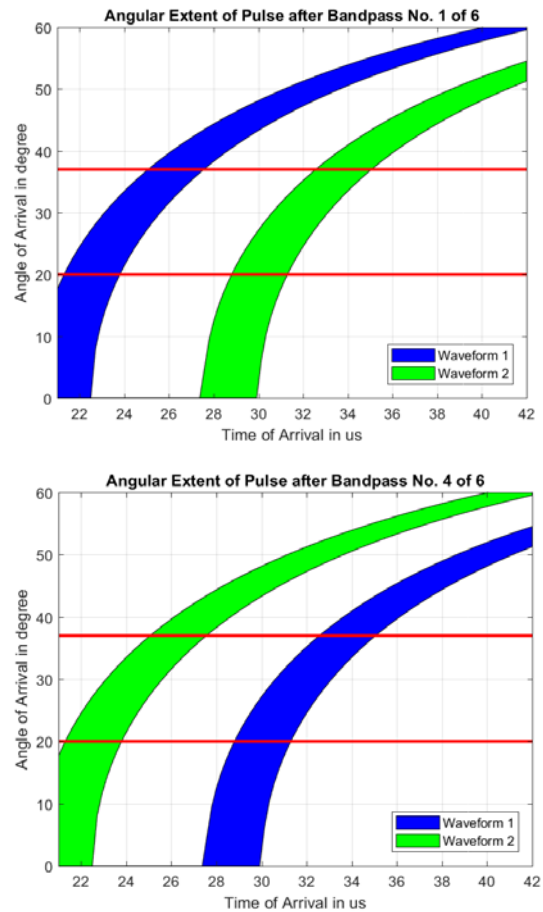


Figure 4 Angle of Arrival (AoA) of the receive signal after the first and the fourth band-pass filters. The lines in red color indicate the position of the swath.

On receive, after acquisition and digital base-band down-conversion of all receive channel raw data, the signal passes a bank of six digital band-pass filters (cf. Figure 3). They are implemented in form of Finite Impulse Response (FIR) filters with the order of 41 taps. The filtering stage divides the full signal bandwidth into six equal-sized sub-bands, which is equivalent to a synthetic narrowing of the total pulse duration. As an illustration, Figure 4 shows the receive signal at the output of the first and of the fourth filter. The blue and green stripes corresponds to the echoes of the first and second Tx waveforms, respectively. The horizontal red lines indicate the angular position of the swath. It can be seen in both graphs of the figure, that the echoes of the band-passed waveforms Tx1 and Tx2 are always separated by $\tau_p/2 = 7.5 \mu\text{s}$.

After filtering, the time-variant receive antenna beams are designed via Linear Constraint Minimum Variance (LCMV) DBF [9] to track the sub-band as it progress over the swath while minimizing interference from the other waveform. This is repeated for all six band-pass filters and implemented for both Tx waveforms individually, yielding 12 time-variant sets of DBF weights. An example for such a receive pattern is plotted in Figure 5. The illuminated swath is indicated by the grey colored bar between 20° and 37° . The bars in red indicate the angle of arrival of the echo from the other side of the aircraft, since the antenna is pointing towards nadir. It can be seen that the pattern after band-pass filter No. 4, at the time of arrival $31.30 \mu\text{s}$, has maximum gain at the Angle of Arrival (AoA) of the first waveform (in blue color), while there is a null at the second waveform (in green color).

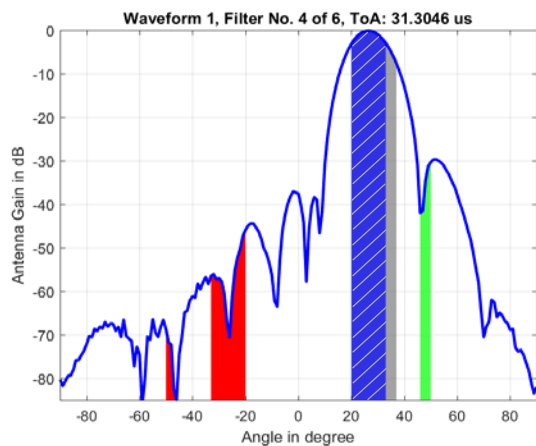


Figure 5 Antenna pattern after DBF for band-pass filter No. 4 at time $31.30 \mu\text{s}$. The echo of the first Tx waveform is preserved, while the echo from the second Tx waveform is suppressed.

The performance of the OWB technique as implemented with DBSAR-2 was evaluated via simulations. A crucial aspect in the technique's performance is high rejection of unwanted energy contributions from the simultaneously transmitted pseudo-orthogonal waveform, and of the echoes from the other side of the aircraft. Also, the strong

nadir returns need to be sufficiently suppressed to avoid receiver saturation. Thus, for each of the six band-pass filters at each time instant, the individual energy contributions on receive were calculated. The results for sub-band No. 4 are presented in Figure 6, where the energy levels from the different unwanted energy contributions are shown as a function of Time of Arrival (ToA).

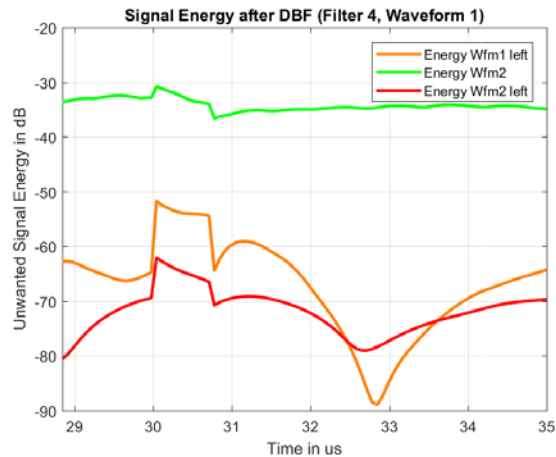


Figure 6 Unwanted energy contributions from second Tx waveform after the time-variant DBF in green color. The orange and red colored curves show the energy from the other side of the aircraft.

As shown in Figure 6, the signal energy is present between ToAs $28.8 \mu\text{s}$ to $35.0 \mu\text{s}$. For other ToAs, there is no expected signal echo in this sub-band and the signal output can therefore be digitally set to zero. It becomes directly apparent, that almost at all ToAs, the second waveform is suppressed by 34 dB or more. Since this value is in the order of the cross-pol coupling of the antenna (35 dB), the simulated result indicates sufficient rejection. It is worth noting that the energy level jump between $30.0 \mu\text{s}$ and $30.8 \mu\text{s}$ is due to the required suppression of nadir echoes. In this time interval, there is a strong unwanted echo from the nadir direction from the first Tx signal. This echo is suppressed by adaptively placing a null in the antenna pattern via the LCMV beamformer. Due to the placement of this null, the antenna pattern gets slightly distorted and the aforementioned energy jump results. The echo signals from the other side of the aircraft are sufficiently suppressed in the simulation in which a homogeneous scene is assumed.

In recent studies, the authors have found out that better waveform suppression can be achieved via the sidelobe constraint DBF technique suggested in [10]. Instead of using the LCMV beamformer, this approach uses adaptive strategies to reach a certain threshold value for the sidelobes of the synthesized pattern. This allows for a control of the complete antenna pattern while avoiding the energy jumps between $30.0 \mu\text{s}$ and $30.8 \mu\text{s}$ in Fig. 6. Results obtained via the sidelobe constraint DBF technique will be presented in a future paper.

4 Summary and Outlook

The orthogonal-waveform beamforming technique is a promising technique for future spaceborne missions since it allows full polarimetric SAR measurements over larger swaths without a degradation of the azimuth resolution, or a reduction of the data rate by a factor of two.

The technique exploits orthogonality properties of signals in order to transmit and receive simultaneously two polarizations. The orthogonality between the polarizations is achieved by the use of SSC waveforms in combination with time-variant DBF in elevation.

The orthogonal-waveform beamforming imaging mode was specified for the DBSAR-2 sensor. Performance simulations with the DBSAR-2 parameters show sufficient suppression of the signal orthogonal components over the full swath.

The technique will soon be tested with DBSAR-2 in an anechoic chamber, and later in a flight campaign. The results will serve as further milestone for the implementation of the technique in a future spaceborne mission.

This work was part of *Collaborative Efforts for Digital Beamforming Synthetic Aperture Radar (CoSAR)* between the National Aeronautics and Space Administration of the United States (NASA) and the German Aerospace Center (DLR).

5 Literature

- [1] J.-H. Kim, M. Younis, A. Moreira and W. Wiesbeck, „Spaceborne MIMO Synthetic Aperture Radar for Multimodal Operation“, *IEEE Transactions on Geoscience and Remote Sensing*, vol. 53, no. 5, pp. 2453-2466, May 2015.
- [2] K. B. Stewart, „Waveform-Diverse Multiple-Input Multiple-Output Radar Imaging Measurements“, Dissertation, Ohio State University, 2016.
- [3] G. Krieger, N. Gebert, M. Younis and A. Moreira, „Advanced Synthetic Aperture Radar Based on Digital Beamforming and Waveform Diversity“, *Proceedings IEEE Radar Conference*, pp. 1-6, May 2008.
- [4] G. Krieger, „MIMO-SAR: Opportunities and Pitfalls“, *IEEE Transactions on Geoscience and Remote Sensing*, vol. 52, no. 5, pp. 2628-2645, May 2014.
- [5] G. Krieger, M. Younis, S. Huber, F. Bordoni, A. Patyuchenko, J.-H. Kim, P. Laskowski, M. Villano, T. Rommel, P. Lopez-Dekker and A. Moreira, „Digital Beamforming and MIMO SAR: Review and New Concepts“, *Proceedings 9th European Conference on Synthetic Aperture Radar, EUSAR*, pp. 11-14, April 2012.
- [6] T. Rommel, M. Younis and G. Krieger, „An orthogonal waveform for fully polarimetric MIMO-SAR“, *Proceedings IEEE Radar Conference*, pp. 887-891, May 2014.
- [7] T. Rommel, M. Younis and G. Krieger, „Demonstration of simultaneous quad-polarization SAR imaging for extended targets in MIMO-SAR“, *Proceedings German Microwave Conference (GeMiC)*, pp. 381-384, 2016.
- [8] R. Rincon, T. Fatoyinbo, B. Osmanoglu, S.-K. Lee, K. J. Ranson, V. Marrero and M. Yeary, „Development of NASA'S Next Generation L-Band Digital Beamforming Synthetic Aperture Radar (DBSAR-2)“, *Proceedings 11th European Conference on Synthetic Aperture Radar (EUSAR)*, pp. 1-4, 6-9 June 2016.
- [9] H. L. Van Trees, „Optimum Array Processing“, ISBN: 978-0471463832: John Wiley & Sons, 2004.
- [10] F. Q. de Almeida, T. Rommel, M. Younis, G. Krieger und A. Moreira, „Multichannel Staggered SAR: System Concepts with Reflector and Planar Antennas“, *IEEE Transactions on Aerospace and Electronic Systems*, accepted for publication, 2018.